

Seasonality of Southern Ocean Sea Ice

ARNOLD L. GORDON

Lamont-Doherty Geological Observatory of Columbia University, Palisades, New York 10964

The sea ice cover of the Southern Ocean undergoes a rapid decrease from mid-November to mid-January. The atmosphere-to-ocean heat flux is insufficient to account for this melting, even in the presence of the high percentage of open water characteristic of the Southern Ocean sea ice. It is estimated that sea-air heat exchange in the 60° to 70°S zone can account for roughly 50% of the required spring heating. The remainder must be supplied by the relatively warm deep water, residing below the Southern Ocean pycnocline. Deep-to-surface water heat flux is accomplished by upwelling of the pycnocline due to the regional Ekman divergence of the surface layer and by cross-pycnocline mixing. It is estimated that the required vertical mixing coefficient for the pycnocline is 1.5 cm²/s. This value is considered as realistic in view of the relatively weak pycnocline which is a consequence of low levels of fresh water input to the surface layer. It is suggested that the magnitude of fresh water input is a major factor in determining the degree of seasonality of Southern Ocean sea ice.

1. INTRODUCTION

The sea ice surrounding Antarctica undergoes large seasonal changes in areal extent. This is evident from both historical observations and recent satellite sensing [Mackintosh, 1946, 1972; Heap, 1964; Zwally and Gloersen, 1977; S. F. Ackley, unpublished manuscript, 1980]. The Zwally *et al.* [1979] review of the sea ice areal cover as observed by satellites for 1973-1975 for greater than 15% and greater than 85% (reproduced as Figure 1) show a sea ice maximum cover in September and October of approximately 20×10^6 km², with a minimum cover in February of approximately 3×10^6 km². Therefore, 17×10^6 km² of sea ice, an area larger than Antarctica, is within the seasonal sea ice zone. As Zwally *et al.* (Figure 1) indicate, much of this cover (about two thirds) has concentrations between 15% and 85% of full ice concentration. If the ice were compacted to 100% concentration, its area would be approximately three fourths of the present cover with leads (C. Parkinson, personal communication, April 1980).

The growth and decay of the sea ice cover shown in Figure 1 for both the 15% and 85% concentration curves are not symmetric about the maximum ice cover. The growth rate is less than the decay rate by nearly a factor of two. The major portion of the decay occurs in the period mid-November to mid-January with a decrease from 17.5×10^6 km² to 6.5×10^6 km². Decay of the greater than 85% cover occurs earlier (mid-October to mid-November) and is even more spectacular in areal decrease, retreating from the near annual maximum cover to only 25% of that in the one month period.

Walsh and Johnson [1979] area versus month plot for Arctic sea ice cover (their Figure 3) shows that the ice growth rate is faster than the ice retreat rate. This contrast with the Southern Ocean situation suggests that fundamental differences exist between the heat budgets of Arctic and Antarctic sea ice.

During the growth period for Southern Ocean sea ice a simple Ekman divergence model yields realistic results [Gordon and Taylor, 1975; S. F. Ackley, unpublished manuscript, 1980]. The concept is as follows: The cyclonic wind field induces a divergent Ekman transport in the surface layer of the ocean. Sea ice on the ocean also diverges, thus generating open water or leads. In the winter when the ocean-atmosphere heat flux is directed towards the atmosphere the leads fill with

new ice. In this way new sea ice forms in the interior of the sea ice fields rather than being accreted to the outer edge. While some addition at the edge may be expected, the northward migration of the ice edge may be primarily governed by the Ekman velocity.

As ice is carried northward, the local heat balance would induce melting, and a steady-state ice cover is attained, as may be the case from August to October. During this period ice forming in the south is balanced by melting in the north. Using Ekman drift velocities presented by Taylor *et al.* [1978], the sea ice northward transport across 60°S amounts to 9.62×10^{13} W poleward heat flux, for each meter thickness of ice.

Ice melting in the spring would also be influenced by Ekman divergence. The atmosphere-to-ocean heat flux would be greatest within the low albedo leads generated by the divergence. The leads act as heat collectors, which accelerate melting of the surrounding pack. Langleben [1972] also stresses the importance of radiational heating within leads in regard to sea ice melting in the Arctic, but points out that radiational heating of the sea ice should not be neglected.

The ability of the sea-air heat flux to account for the spring retreat of the sea ice is now tested. The ice charts of the Navy-NOAA ice center indicate that during the mid-November to mid-January period sea ice virtually disappears over the deep ocean. The additional ice melt from mid-January to mid-February is mainly over the continental margins of Antarctica. The major exception is the 0.8×10^6 km² (about one third of which is over the deep ocean) field of perennial sea ice east of the Antarctic Peninsula.

Southern Ocean seasonal sea ice is estimated at 1.0 to 1.5 m [Untersteiner, 1966]. The heat required to melt the average sea ice thickness of 1.25 m with a latent heat of fusion of 292 J/g (Table 4.3 from Neumann and Pierson [1966]) is 3.3×10^8 J/m². Since most of the open ocean ice is removed in the 60-day period from mid-November to mid-January, the daily heat requirement is 552×10^4 J/m² d or 64 W/m². This represents a minimum heat requirement since a higher value would be necessary if significant warming of the surface water occurs before mid-January or if the heat required to melt icebergs is taken into account. While some warming is observed, and icebergs melting in early summer occurs, both are neglected in the calculations. The question is: Can the atmosphere-to-ocean heat flux provide enough heat to explain the sea ice decay even if no other demands are placed on the available heat?

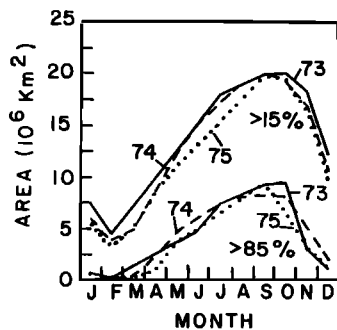


Fig. 1. Areal extent of Southern Ocean waters with sea ice concentration at least 15% and with sea ice concentration at least 85% in 1973, 1974, and 1975 [Zwally *et al.*, 1979].

2. SEA-AIR HEAT EXCHANGE IN THE BAND 60°–70°S

Estimates for sea-air heat exchange for the 60°–70°S latitude band are made using monthly climatic data (Table 1) for ice free (Table 2), full ice and partial ice cover (Table 3). Admittedly, the errors associated with these calculations are large, due to inadequate meteorological data set, use of monthly means rather than shorter term means, uncertainty in the exchange coefficients for the non-radiative heat flux terms and from uncertainty in the exact amount of sea ice insulation of the ocean (the R term in Table 3) and ratio of ice cover to open ocean (P value in Table 3).

The required poleward oceanic heat across 60°S for balance of ocean heat loss between 60°–70°S (16.8×10^{16} cm²) is determined for each of the ice concentration situations (Table 4). Oceanic heat flux across 60°S estimated by *Hastenrath* [1980] is 13×10^{13} W. Hastenrath's heat flux estimate across 53°S, which marks the mean circumpolar position of the polar front, is 35×10^{13} W (his Figure 9), similar to the value suggested by *Gordon* [1975]. It is surprising that his 60°S value is so much lower than his 53°S value. It implies large ocean heat loss in the 53°–60°S zone (13 W/m²) where other estimates [see *Taylor et al.*, 1978] actually suggest a small annual heat gain by the ocean in this zone. His heat flux value across 60°S is low by a factor of 4 compared to the value given in Table 4 for realistic ice cover, but is close to the full ice cover condi-

TABLE 1. Meteorological Parameters Used to Calculate Sea-Air Heat Exchange Within 60°–70°S

Month	T_s , °C	T_a , °C	T_d , °C	W , m/s	C
January	1	0	-3	3	0.75
February	1	-1	-4	3	0.75
March	0	-2	-5	3	0.75
April	0	-5	-8	4	0.75
May	-2	-8	-10	4	0.75
June	-2	-10	-13	4	0.75
July	-2	-12	-14	4	0.75
August	-2	-12	-14	4	0.75
September	-2	-11	-13	4	0.75
October	-2	-7	-11	4	0.75
November	-2	-4	-7	4	0.75
December	0	-1	-5	3	0.75

T_s , sea surface temperature (summer values from historical data; values during sea ice months taken as nearest whole degree to freezing). T_a , air temperature (average at 65°S from *Taljaard et al.* [1969]). T_d , dew point temperature (average at 65°S from *Taljaard et al.* [1969]). W , wind speed (average at 65°S from *Jenne et al.* [1971]). C , cloud cover (75% cover all year, from Table 2.2 of *Sasamori et al.* [1972]).

tion. *Trenberth* [1979], on the other hand, determines a 100×10^{13} W flux across 60°S, closer to the open ocean value and about twice that for the realistic sea ice condition (Table 4). *Newton* [1972, Appendix C] gives 29.3×10^{13} W ocean heat flux across 60°S, approximately twice Hastenrath's value, half of the Table 4 value for realistic ice cover, and one third of *Trenberth's* values.

The one order of magnitude range in heat flux estimates across 60°S indicates some of the difficulties in determining this important number. Before it is possible to identify the primary mechanism responsible for meridional heat flux in the Southern Ocean, it is necessary to establish reliable sea-air heat flux estimates as a function of latitude for the Southern Ocean. In this present study the mode in which the heat flux into the 60°–70°S zone is accomplished is important only in that it is assumed the annual heat loss of the surface water to the atmosphere is balanced by vertical heat transfer across the pycnocline, rather than lateral poleward heat transfer within the surface layer itself. Since the Ekman drift is directed towards the equator, this assumption is justified.

3. DISCUSSION

It is unlikely that the atmosphere-to-ocean heat flux given in Tables 2 and 3 is adequate to account for the massive ice melt from mid-November to mid-January. For the realistic ice cover the average heat gain for this period is 34 W/m², slightly over 50% of the required minimum heat flux. Even the higher estimate of 47 W/m² for a no-ice condition is not sufficient and the full ice cover value of 7 W/m² is grossly insufficient. This suggests two things: leads induced by the general Ekman divergence must be an important factor by increasing ocean warming to a point where atmosphere-to-ocean heat flux can play more than a minor role in the spring ice cover retreat and that an additional source of heat is needed to balance the surface water heat balance during the spring melting as well as on an annual basis (both values are about 30 W/m²).

Heat flux into the surface layer from the sub-pycnocline water is the probable source of this heat. Sub-pycnocline water is significantly warmer than the surface water (Figure 2) and forms an effective heat (and salt) reservoir. Deep water heat can be introduced into the surface layer by the general upwelling of the pycnocline expected from the climatic Ekman divergence and by cross-pycnocline heat flux by turbulence and possibly convective processes, which can be parameterized by a K_z (vertical mixing coefficient).

The Ekman induced upwelling in the 60°–70°S band estimated by *Taylor* [1978] (also see *Gordon et al.* [1977], *Taylor et al.* [1978]) is 1×10^{-4} cm/s. Since the deep water is approximately 3°C warmer than the winter surface water, Ekman pumping could provide about 13 W/m². Since both the total annual as well as average mid-November to mid-January deep water contribution to the surface layer is expected to be 31 W/m², about 18 W/m² must be derived from the vertical diffusive and/or convective heat flux ($\rho C_p K_z \Delta T / \Delta Z$). This requires a ρK_z value of 1.5 cm²/s (using a pycnocline thermal gradient of 3×10^{-4} °C/cm).

The annual average vertical flux of heat by Ekman pumping and vertical mixing effects would provide on a daily basis, about 50% of the required mid-November to mid-January heat. This amount together with the atmosphere to ocean heat flux can satisfy the heat required to explain the spring sea ice melting.

TABLE 2. Average Monthly Heat Flux Into Ocean 60°–70°S for Ice-Free Conditions (Values in W/m² and cal/cm² d)

Month	Q_s	Q_b	Q_h	Q_e	Q_{io}
January	162 [335]	35 [72]	7 [15]	39 [81]	81 [167]
February	109 [225]	36 [74]	15 [31]	47 [98]	11 [22]
March	56 [116]	36 [74]	15 [31]	44 [91]	-39 [-80]
April	21 [43]	36 [75]	50 [104]	72 [149]	-138 [-285]
May	12 [24]	36 [74]	60 [124]	63 [131]	-148 [-305]
June	4 [8]	36 [74]	80 [165]	66 [137]	-178 [-368]
July	2 [5]	36 [75]	100 [207]	72 [149]	-206 [-426]
August	38 [78]	36 [75]	100 [207]	72 [149]	-171 [-353]
September	76 [156]	36 [74]	90 [186]	68 [140]	-118 [-244]
October	106 [219]	36 [74]	50 [103]	69 [143]	-49 [-101]
November	128 [265]	35 [73]	20 [41]	60 [124]	13 [27]
December	142 [294]	36 [75]	8 [16]	52 [107]	47 [97]
Average	71 [147]	36 [74]	49 [102]	61 [125]	-75 [-154] -56.2 kcal/cm ² yr

Q_s , incoming solar radiation absorbed by ocean 60°–70°S from values given by *Sasamori et al.* [1972, Tables 2.6 to 2.9] interpolated to each month with an ocean surface albedo of 10% for the direct radiation and 6.6% for the diffuse radiation. Q_b , net back radiation where cloud cover (in tenths) is assumed to be middle level clouds (equation from *Reed* [1976]). Q_h , sensible heat exchange (equation from *Budyko* [1963]). Q_e , evaporative heat exchange (equation from *Budyko* [1963]). Q_{io} , net sea-air transfer for ice-free ocean: $Q_{io} = Q_s - Q_b - Q_h - Q_e$.

A ρK_z value of 1.5, though large for an oceanic main pycnocline, may be appropriate for the weak stability characteristic of the Southern Ocean pycnocline south of the polar front. *Sarmiento et al.* [1976] using radon distribution within the abyssal ocean show that vertical mixing coefficient bears an inverse relationship to the buoyancy gradient, suggesting a constant buoyancy flux. The Southern Ocean pycnocline, while stronger than the vertical density gradient of the abyssal ocean, is markedly weaker than the main pycnocline of the world ocean. The maximum buoyancy gradient below the temperature minimum layer, which represents the base of the winter mixed layer, around Antarctica at 65°S (determined from the data given in the Southern Ocean Atlas by *Gordon et al.* [1981] falls in the range of 350 to $3400 \times 10^{-8} \text{ s}^{-2}$ with an average of $1300 \times 10^{-8} \text{ s}^{-2}$. This range with a K_z of 1.5, plotted on the *Sarmiento et al.* relation (Figure 3) falls toward the

high end of the envelope, but in view of the greater shear expected within the shallow Southern Ocean pycnocline relative to the abyssal ocean, the 1.5 K_z value is not unreasonable, particularly if convective events occur [*Gordon*, 1978; *Killworth*, 1979].

The above calculations suggest that sea ice melting in the mid-November to mid-January period is facilitated by Ekman layer generation of leads which act as radiative heat collectors and by deep water to surface water heat flux due to Ekman upwelling and cross-pycnocline mixing processes. While it is possible, in view of the uncertainty in the sea-air heat exchange calculations that the lead generation mechanism alone is sufficient to account for the melting, the possibility of a significant role of cross-pycnocline heat flux must be considered particularly since the required K_z value is not unreasonable. It is expected that cross-pycnocline processes would be most important at the end of the ice growth period when (1) the cumulative effects of winter sea ice formation induce the yearly maximum in surface water salinity (and density), and (2) the insulating effect of the sea ice may act to trap the deep water heat flux in the surface layer [*Welander*, 1977].

Parkinson and Washington [1979] require a substantial ocean to ice heat flux to induce spring melt back. They use a value of 25 W/m^2 , about one order magnitude higher than the value used in the Arctic. Use of the Arctic value for the Southern Ocean did not result in the spring melt back. Use of a value of 40 W/m^2 did not allow for winter sea ice formation (*C. Parkinson*, personal communication, June 1980). Thus modelling attempts have difficulty in producing the intense seasonality of Southern Ocean sea ice, without resorting to vertical flux of the deep ocean heat.

TABLE 3. Average Monthly Heat Flux Into Ocean for Full and Partial Ice Cover (Values in W/m² and cal/cm² d)

Month	R	Q_{ii}	P	Q_i
January	0.36	29 (60)	0.3	65 (135)
February	0.28	3 (6)	0.1	10 (20)
March	0.20	-8 (-16)	0.2	-32 (-67)
April	0.23	-32 (-66)	0.4	-95 (-197)
May	0.17	-25 (-52)	0.5	-87 (-179)
June	0.12	-21 (-44)	0.6	-84 (-174)
July	0.12	-25 (-51)	0.7	-79 (-164)
August	0.09	-16 (-32)	0.7	-62 (-128)
September	0.07	-8 (-17)	0.8	-30 (-62)
October	0.15	-7 (-15)	0.7	-20 (-41)
November	0.14	2 (4)	0.6	6 (13)
December	0.27	13 (26)	0.4	33 (68)
Average		-8 (-16) 5.8 kcal/cm ² yr		-31 (-65) -24 kcal/cm ² yr

R , ratio of heat flux with full ice cover to heat flux for no ice cover. Determined from data presented in Figures A-8 and A-10 of *Fletcher* [1969]. (See section III-B of *Hibler* [1979] for a discussion of the thermal processes in sea ice.) Q_{ii} , net sea-air heat transfer for full sea ice cover. P , proportion of 60°–70°S covered with sea ice (estimated from the Navy-NOAA charts). Q_i , net sea-air heat flux for realistic sea ice-open ocean ratio or the 60°–70°S belt.

TABLE 4. Annual Average Heat Flux Across 60°S to Balance 60°–70°S Ocean Heat Loss to the Atmosphere

Condition	Watts	Cal/s
1. Ice free	130×10^{13}	31×10^{13}
2. Total ice cover	13×10^{13}	3×10^{13}
3. Realistic ice cover	54×10^{13}	13×10^{13}

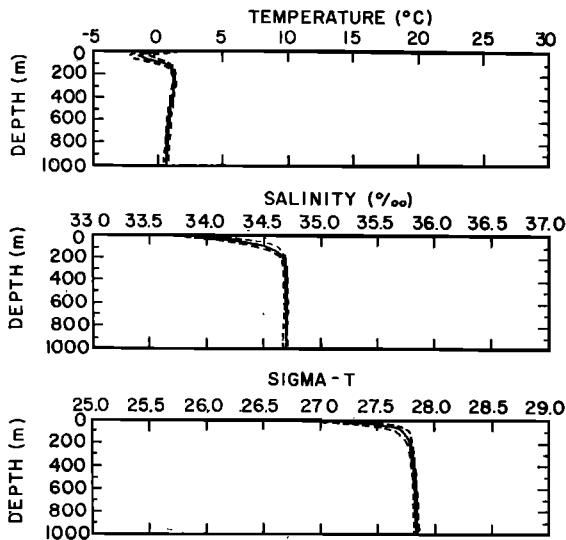


Fig. 2. An example of thermohaline stratification in the seasonal sea ice zone of the Southern Ocean. The plot shows the mean temperature (degrees Centigrade), salinity (per mil), and sigma- t (density anomaly) versus depth at 65°S, 20°E. The envelope around the central curve indicates range in parameters. This plot is taken from the microfiche supplement to the *Southern Ocean Atlas* by Gordon et al. [1981].

Stommel [1980], using vertical temperature-salinity curves between Australia and Antarctica (35°–60°S) and the estimates of meridional heat and fresh water flux [Hastenrath, 1980; Baumgartner and Reichel, 1925], determines the required water mass flux across latitudes, as well as the spreading pattern. Across 60°S Stommel finds a required poleward flux of warm, salty deep water of $18 \times 10^6 \text{ m}^3/\text{s}$, with a circulation pattern similar to that proposed by Deacon [1937]: deep water converted by sea-air exchange into antarctic surface water returns northward at depths shallower than the deep water poleward migration. Using the larger 60°S heat flux value presented in this paper (about 2.5 larger than the value used by Stommel), the required deep water flux would increase correspondingly and the mode of the exchange would be more isopycnal. It is noted that the southern end of the Deacon pattern, in which the altered deep water spreads northward as

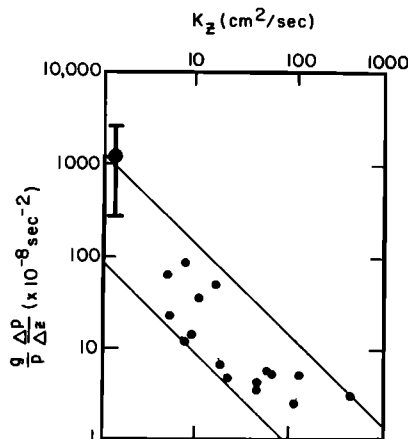


Fig. 3. Relation of the K_z to buoyancy gradient. The dots are taken from Sarmiento et al. [1976], based upon Radon measurements in the abyssal ocean. The mean value for K_z determined for the Southern Ocean pycnocline is given by the large dot with the range of buoyancy gradient along 65°S given by the vertical line.

antarctic bottom water are not included in Stommel's results. Perhaps use of the hydrographic data south of 60°S, particularly in the Weddell region, might have revealed this regime.

4. ROLE OF PRECIPITATION

The weak Southern Ocean pycnocline is a consequence of the relatively high salinity of the surface water due to the small fresh water input. Estimates of precipitation minus evaporation ($P - E$) summarized by Newton [1972, Figure 9.14] for 60°–70°S are 0.075 cm/d, or 27 cm/yr. Baumgartner and Reichel [1975] arrive at a value of 32 cm/yr. Continental runoff (in the form of icebergs) contribution to the 60° to 70°S ocean area can be taken as 10 cm/yr (since the ocean area is about 15% larger than Antarctica, which has a mean precipitation of 11 to 19 cm/yr [Van Loon, 1972]); so the total fresh water flux (F) is taken about 40 cm/yr. This value, when used with estimates of ocean heat loss to the atmosphere, 31 W/m^2 (Table 3), can be used to determine the path followed in temperature-salinity space by a parcel of water exposed to the atmosphere. The $\Delta T/\Delta S$ slope is given by (so is the initial salinity of the water parcel)

$$\frac{\Delta T}{\Delta S} = \frac{Q_T/\rho C_p}{S_0 F} = 18.0^\circ\text{C}/\text{‰}$$

Since the $\Delta T/\Delta S$ slope of an isopycnal in the -2 to $+2^\circ\text{C}$ temperature range is $15.4^\circ\text{C}/\text{‰}$, the thermohaline alteration of deep water which becomes incorporated into the surface layer would follow a T/S path which would increase its density with time. Therefore, thermohaline alteration in the 60°–70°S belt induces an unstable boundary between deep water and surface water or, at best, a marginally stable stratification. It is possible that fresh water input would be further in deficit if sea ice is removed from the 60°–70°S band at a more rapid rate than the surface water by Ekman drift.

In view of the errors associated with the heat and fresh water flux, it can be concluded that low stability of the Southern Ocean pycnocline is a consequence of a relatively low fresh water input which nearly balances the thermal buoyancy flux. This is in strong contrast to the high fresh water input into the Arctic, which induces a strong pycnocline:

Variations in $P - E$ have a strong impact on the pycnocline stability and hence on the K_z value and vertical heat flux. Increased $P - E$ would lead to higher vertical stability with less spring ice melt, while decreased $P - E$ would increase vertical processes and lead to more rapid ice removal in the spring. Thus the seasonality of Southern Ocean sea ice may depend on precipitation in addition to the obvious dependence on the heat budget. Perhaps the significant variations in the degree of seasonality of the Southern Ocean sea ice which have occurred in the geological past [Cooke and Hayes, 1980] are a consequence of pycnocline stability variations.

Another manifestation of the cross-pycnocline heat flux is the Weddell Polynya. The polynya is most likely the consequence of enhanced vertical heat flux by convective events induced by a severe weakening or complete break-down of the pycnocline [Gordon, 1978; Killworth, 1979; Martinson et al., 1981]. In this way it represents a more dramatic form of the processes which initiate the rapid spring melt of the Southern Ocean sea ice.

Stability of the Southern Ocean pycnocline would be increased if cross-pycnocline heat and salt flux is influenced by the diffusive case of double diffusion [Turner, 1973]. In this

process less salt is transferred upward than would be the situation for a conservative exchange process. Middleton and Foster [1980] using observed fine structure in the Weddell Sea pycnocline and results from laboratory experiments for double diffusion find the ratio of salinity to heat flux is 0.048. A value of 0.166 is expected for a conservative exchange process. Thus, a double diffusion process will supply only 29% of the salinity flux expected for a conservative mixing process. However, the magnitude of the double diffusive fluxes determined by Middleton and Foster are about one order of magnitude less than the required annual sea-air heat and salt flux.

5. CONCLUSIONS

Upward heat flux into the 60°–70°S surface water is required to balance not only the annual sea-to-air heat transfer, but also to account for the rapid decrease of the sea ice cover during the mid-November to mid-January period. The vertical heat flux is accomplished by both upwelling induced by Ekman divergence of surface water and cross-pycnocline mixing. The latter is significant because of the low input of fresh water into the surface layer. Thus it is probable that the Southern Ocean sea ice seasonality can be attributed to the Ekman divergence (which also influences sea-air exchange) and to an inherently weak pycnocline.

Acknowledgments. The Southern Ocean research of the author is supported by National Science Foundation grant DPP 78-24832. I thank one of the reviewers of this manuscript who pointed out the existence of the Stommel study. I thank S. Ackley for supplying a preprint of his presentation at the 1979 IUGG meeting in Canberra, Australia, and for pointing out the significance of freshwater removal by sea ice transport. Lamont-Doherty Geological Observatory contribution 3121.

REFERENCES

- Baumgartner, A., and E. Reichel, *The World Water Balance*, 179 pp., Elsevier, New York, 1925.
- Budyko, M. I., *Atlas Teplovogo Balansa Zemnogo Shara*, 69 pp., Akademiya Nauk SSSR, Moscow, 1963.
- Cooke, D. W., and J. D. Hayes, Estimates of Antarctic seasonal ice cover during glacial intervals, in *Proceedings of the Third Symposium on Antarctic Geology and Geophysics, August 21–26, 1977*, in press, 1980.
- Deacon, G. E. R., The hydrology of the Southern Ocean, *Discovery Rep.*, 15, 1–124, 1937.
- Fletcher, J. O., Ice extent on the Southern Ocean and its relationship to world climate, *Memo. RM-5793-NSF*, 108 pp., Rand Corp., Santa Monica, Calif., 1969.
- Gordon, A. L., General ocean circulation, in *Numerical Models of Ocean Circulation*, pp. 39–53; National Academy of Sciences, Washington, D. C., 1975.
- Gordon, A. L., Deep Antarctic convection west of Maud Rise, *J. Phys. Oceanogr.*, 8, 600–612, 1978.
- Gordon, A. L., and H. Taylor, Seasonal change of Antarctic sea ice cover, *Science*, 187, 346–347, 1975.
- Gordon, A. L., H. W. Taylor, and D. T. Georgi, Antarctic oceanographic zonation, in *Polar Oceans*, edited by M. J. Dunbar, pp. 45–76. Arctic Institute of North America, Calgary, Alta., 1977.
- Gordon, A. L., E. Molinelli, and T. Baker, *Southern Ocean Atlas*, Columbia University Press, New York, in press, 1981.
- Hastenrath, S., Heat budget of tropical ocean and atmosphere, *J. Phys. Oceanogr.*, 10(2), 159–170, 1980.
- Heap, J. A., Pack ice, in *Antarctic Research*, edited by R. Priestly, R. J. Aidié, and G. de Q. Robin, pp. 308–317, Butterworths, London, 1964.
- Hibler, W. D., III, A dynamic-thermodynamic sea ice model, *J. Phys. Oceanogr.*, 9(4), 815–846, 1979.
- Jenne, R. L., H. L. Crutcher, H. Van Loon, and J. J. Taljaard, Climate of the upper air: Southern hemisphere, III, Vector mean geostrophic winds, isogon and isotach analyses, *NCAR-TN/STR-58*, Nat. Center for Atmos. Res., Boulder, Colo., 1971.
- Killworth, P. D., On 'chimney' formations in the ocean, *J. Phys. Oceanogr.*, 9, 531–554, 1979.
- Langleben, M. P., The decay of an annual cover of sea ice, *J. Glaciol.*, 11, 337–344, 1972.
- Mackintosh, N. A., The Antarctic Convergence and the distribution of surface temperatures in Antarctic waters, *Discovery Rep.*, 23, 177–212, 1946.
- Mackintosh, N. A., Life cycle of Antarctic krill in relation to ice and water conditions, *Discovery Rep.*, 36, 94 pp., 1972.
- Martinson, D. G., P. D. Killworth, and A. L. Gordon, A convective model for the Weddell Polynya, *J. Phys. Oceanogr.*, in press, 1981.
- Middleton, J. H., and T. D. Foster, Fine structure measurements in a temperature-compensated halocline, *J. Geophys. Res.*, 85(C2), 1107–1122, 1980.
- Neumann, G., and W. J. Pierson, *Principles of Physical Oceanography*, 545 pp., Prentice-Hall, Englewood Cliffs, N. J., 1966.
- Newton, C. W., Southern hemisphere general circulation in relation to global energy and momentum balance requirements, in *Meteorology of the Southern Hemisphere*, *Meteorol. Monogr.* 13, pp. 215–246, American Meteorological Society, Boston, Mass., 1972.
- Parkinson, C. L., and W. M. Washington, A large-scale numerical model of sea ice, *J. Geophys. Res.*, 84, 311–337, 1979.
- Reed, R. K., On estimation of net longwave radiation from the oceans, *J. Geophys. Res.*, 81(33), 5793–5794, 1976.
- Sarmiento, J. L., H. W. Geely, W. S. Moore, A. E. Bainbridge, and W. S. Broecker, The relationship between vertical eddy diffusion and buoyancy gradient in the deep sea, *Earth Planet. Sci. Lett.*, 32, 357–370, 1976.
- Sasamori, T., J. London, and D. V. Hoyt, Radiation budget of the southern hemisphere, in *Meteorology of the Southern Hemisphere*, vol. 13, pp. 9–23, American Meteorological Society, Boston, Mass., 1972.
- Stommel, H., How the ratio of meridional flux of fresh water to flux of heat fixes the latitude where low salinity intermediate water sinks, *Tellus*, 32(6), 562–566, 1980.
- Taljaard, J. J., H. Van Loon, H. L. Crutcher, and R. L. Jenne, Climate of the upper air: Southern hemisphere, I, Nat. Center for Atmos. Res., Boulder, Colo., 1969.
- Taylor, H. W., Some large aspects of the Southern Ocean and its environment, Ph.D. thesis, Columbia Univ., New York, 1978.
- Taylor, H. W., A. L. Gordon, and E. Molinelli, Climatic characteristics of the Antarctic Polar Front Zone, *J. Geophys. Res.*, 83, 4572–4578, 1978.
- Trenberth, K. E., Mean annual poleward energy transport by the oceans in the southern hemisphere, *Dyn. Atmos. Ocean*, 4, 57–64, 1979.
- Turner, J. S., *Buoyancy Effects in Fluids*, 367 pp., Cambridge University Press, New York, 1973.
- Untersteiner, N., Sea ice, in *Encyclopedia of Oceanography*, edited by R. W. Fairbridge, 1021 pp., Reinhold, New York, 1966.
- Van Loon, H., Cloudiness and precipitation in the southern hemisphere, in *Meteorology of the Southern Hemisphere*, *Meteorol. Monogr.* 13, pp. 101–112, American Meteorological Society, Boston, Mass., 1972.
- Walsh, J. E., and C. M. Johnson, An analysis of Arctic Sea ice fluctuations, 1953–77, *J. Phys. Oceanogr.*, 9(3), 580–591, 1979.
- Welander, P., Observation of oscillatory ice states in a simple convection experiment, *J. Geophys. Res.*, 82(18), 2591–2592, 1977.
- Zwally, H. J., and P. Gloersen, Passive microwave images of the polar regions and research applications, *Polar Rec.*, 18(116), 431–450, 1977.
- Zwally, H. J., C. Parkinson, F. Carsey, P. Gloersen, W. J. Campbell, and R. O. Ramseier, Antarctic sea ice variations 1973–75, in *NASA Weather Climate Review*, Pap. 56, pp. 335–340, National Aeronautics and Space Administration, Washington, D. C., 1979.

(Received July 25, 1980;
revised November 10, 1980;
accepted November 12, 1980.)